Capacity and Delay Analysis of Next-Generation Passive Optical Networks (NG-PONs)

Frank Aurzada, Michael Scheutzow, Martin Reisslein, *Senior Member, IEEE,*
Navid Ghazisaidi, and Martin Maier, *Senior Member, IEEE*

***Abstract*—Building on the Ethernet Passive Optical Network (EPON) and Gigabit PON (GPON) standards, Next-Generation (NG) PONs (i) provide increased data rates, split ratios, wavelengths counts, and fiber lengths, as well as (ii) allow for all-optical integration of access and metro networks. In this paper we provide a comprehensive probabilistic analysis of the capacity (maximum mean packet throughput) and packet delay of subnetworks that can be used to form NG-PONs. Our analysis can cover a wide range of NG-PONs through taking the minimum capacity of the subnetworks forming the NG-PON and weighing the packet delays of the subnetworks. Our numerical and simulation results indicate that our analysis quite accurately characterizes the throughput-delay performance of EPON/GPON tree networks, including networks upgraded with higher data rates and wavelength counts. Our analysis also characterizes the trade-offs and bottlenecks when integrating EPON/GPON tree networks across a metro area with a ring, a Passive Star Coupler (PSC), or an Arrayed Waveguide Grating (AWG) for uniform and non-uniform traffic. To the best of our knowledge, the presented analysis is the first to consider multiple PONs interconnected via a metro network.**

***Index Terms*—Metro area network, packet delay, passive optical network, throughput-delay analysis.**

I. Introduction

THE Passive Optical Network (PON) is one of the most widely deployed access networks due to its unique benefits, including transparency against data rate and signal format as well as high data rates and reliability [1]. The two major state-of-the-art PON standards IEEE 802.3ah Ethernet PON (EPON) and ITU-T G.984 Gigabit PON (GPON) consist both of a single upstream wavelength channel and a separate single downstream wavelength channel, whereby both channels are operated with time division multiplexing (TDM). EPON and GPON are expected to coexist for the foreseeable future as they evolve into Next-Generation PONs (NG-PONs). NG-PONs are mainly envisioned to (i) achieve higher performance parameters, e.g., higher bandwidth per subscriber, increased split ratio, and extended maximum reach, than current EPON/GPON architectures [2], and (ii) broaden EPON/GPON functionalities to include, for instance, the consolidation of optical access, metro, and backhaul networks as well as the support of topologies other than conventional tree structures [3].

In this paper, we evaluate the capacity (maximum mean packet throughput) and packet delay of a wide range of NG-PONs through probabilistic analysis and verifying simulations. More specifically, we analyze the capacity and delay of various subnetworks from which NG-PONs can be formed, thus enabling analytical capacity and delay characterization for a wide range of NG-PONs built from the examined subnetworks. Two important applications for our analysis are: (A) The obtained results provide insight into the performance limitations of candidate NG-PON architectures and thus inform network operators seeking to upgrade their installed TDM PONs. (B) Neither IEEE 802.3ah EPON nor ITU-T G.984 GPON standardizes a specific dynamic bandwidth allocation (DBA) algorithm. The design of DBA algorithms is left to manufacturers which aim at equipping network operators with programmable DBA algorithms that adapt to new applications and business models and thus make PONs future-proof. Our capacity and delay analysis provides an upper throughput bound and a delay benchmark for polling-based medium access control with gated service [4] which can be used to evaluate the throughput-delay performance of current and future DBA algorithms for NG-PONs.

This paper is structured as follows. In the following section, we review related work on the analysis of PON access and metro packet networks. In Section III we give overviews of the EPON and GPON access networks. In Section IV, we present NG-PONs that either (i) upgrade PONs or (ii) interconnect multiple PONs across a metropolitan area. We conduct the capacity and delay analysis of the subnetworks forming NG-PONs in Section V. In Section VI, we compare numerical throughput-delay results obtained from our analysis with simulations and illustrate the application of our capacity analysis to identify bottlenecks in NG-PONs. We briefly summarize our contributions in Section VII.

II. Related Work

In this section we briefly review related work on the analysis of passive optical networks and metropolitan area networks.

Paper approved by J. A. Salehi, the Editor for Optical CDMA of the IEEE Communications Society. Manuscript received July 19, 2010; revised October 15, 2010.

F. Aurzada and M. Scheutzow are with the Department of Mathematics, Technical University Berlin, 10623 Berlin, Germany (e-mail: {aurzada, ms}@math.tu-berlin.de).

M. Reisslein is with the School of Electrical, Computer, and Energy Engineering, Arizona State University, Tempe, Arizona 85287-5706, USA (e-mail: reisslein@asu.edu).

N. Ghazisaidi was with the Optical Zeitgeist Laboratory, INRS, University of Québec. He is now with Ericsson Inc., 200 Holger Way, CA 95134, San Jose, USA (e-mail: navid.ghazisaidi@ericsson.com).

M. Maier is with the Optical Zeitgeist Laboratory, INRS, University of Québec, Montréal, QC, H5A 1K6, Canada (e-mail: maier@emt.inrs.ca).

Supported by the DFG Research Center Matheon "Mathematics for key technologies" in Berlin.

Digital Object Identifier 10.1109/TCOMM.2011.030411.100418

EPONs employ medium access control with an underlying polling structure [5]. Building directly on the literature on polling systems, e.g., [6], Park et al. [7] analyze an EPON model with random independent switchover times. This EPON model holds only when successive upstream transmissions are separated by a random time interval sufficiently large to "decorrelate" successive transmissions, which would significantly reduce bandwidth utilization in practice. In an EPON, the service (upstream transmission) of an Optical Network Unit (ONU) follows immediately (separated by a guard time) after the upstream transmission of the preceding ONU to ensure high utilization. The switchover time is therefore generally highly dependent on the round-trip delays and the masking of the round-trip delays through the interleaving of upstream transmissions [4]. Subsequent analyses have strived to model these correlated transmissions and switchovers with increasing fidelity [8]–[11].

GPONs have received relatively less research interest than EPONs. To the best of our knowledge we conduct the first delay analysis of GPONs in this paper. Similarly, WDM PONs have received relatively little research attention to date. The call-level performance of a WDM PON employing Optical Code Division Multiple Access (OCDMA) [12] was analyzed in [13]. To the best of our knowledge packet-level analyses of WDM EPONs has so far only been attempted in [14, Section 2.4] where an WDM EPON with offline scheduling (also known as interleaved polling with stop [5]) was analyzed and in [15], [16] where the capacity of WDM PONs was examined. In contrast, we analyze in this paper the capacity and packet delay for WDM PON channels operating in online-scheduling PONs that are integrated with metro networks.

Metropolitan area networks have received significant attention over the past two decades. The capacity and delay performance of packet ring networks with a variety of MAC protocols has been analyzed in numerous studies, see e.g., [17]. The impact of fiber shortcuts in ring networks has been analyzed in [18]. In this paper, we analyze to the best of our knowledge for the first time a comprehensive NG-PON that interconnects multiple PONs via a metro network combining a ring and star networks.

III. Overview of EPON and GPON

Typically, both EPON and GPON have a physical tree topology with the OLT at the root [19]. The OLT connects through an optical splitter to multiple ONUs, also known as Optical Network Terminals (ONTs). Each ONU can serve a single or multiple subscribers. To facilitate DBA, both EPON and GPON use polling based on a *report/grant mechanism*. In each polling cycle, ONUs send their instantaneous upstream bandwidth demands through report messages to the OLT, which in turn dynamically allocates variable upstream transmission windows by sending a separate grant message to each ONU.

The EPON is a symmetric network providing a data rate of 1 Gb/s in both upstream and downstream directions. It provides a reach between OLT and ONUs of up to 20 km for a split ratio initially set to 1:16 [19], [20] and recently reaching 1:64 [21]. The EPON has variable-length polling cycles based on the bandwidth demands, which are signalled with the multipoint control protocol (MPCP). The ONU uses the MPCP REPORT message to report bandwidth requirements to the OLT. The OLT passes received REPORT messages to its DBA algorithm module to calculate the upstream transmission schedule [5]. Then, the OLT issues upstream transmission grants by transmitting a GATE message specifying the start time and length of the transmission window to each ONU. The transmission window may comprise multiple Ethernet frames, whereby EPON does not allow for fragmentation. EPON carries Ethernet frames natively, i.e., without encapsulation.

The GPON offers several combinations of upstream/downstream data rates with a preferred rate of 2.488 Gb/s downstream and 1.244 Gb/s upstream for up to 60 km reach and a maximum split ratio of 1:128 [19], [21]. Both upstream and downstream transmissions are based on a periodically recurring time structure with a fixed frame length of $\delta = 125\ \mu$s. Each upstream frame contains dynamic bandwidth report (DBRu) fields. Each downstream frame contains a physical control block (PCBd), which includes a bandwidth map (BWmap) field specifying the ONU upstream transmission grants. Unlike the EPON, the GPON deploys the GPON encapsulation method (GEM) involving a 5-byte GEM header and allows for Ethernet frame fragmentation. Two DBA methods are defined for GPON: (i) status-reporting DBA based on ONU reports via the DBRu field, and (ii) non-status-reporting DBA based on traffic monitoring at the OLT. Recent GPON research has focused on the design and evaluation of status-reporting DBA algorithms [22]. The impact of the various types of guard times and overhead fields on the bandwidth efficiency of both EPON and GPON has been thoroughly investigated in [23], [24].

IV. NG-PONs

Generally, NG-PON technologies fall into two categories [25]: (i) Evolutionary NG-PON technologies provide improved performance, such as higher data rates, with legacy optical distribution networks and co-exist with legacy PONs. (ii) Revolutionary (disruptive) NG-PON technologies, such as optical code division multiplexing (OCDM), provide enhanced services on new distribution networks. We focus on evolutionary NG-PON technologies that are expected to replace current state-of-the-art GPON and EPON solutions in the near- to mid-term.

A. High-speed TDM PON

Higher speeds are needed to support emerging bandwidth-hungry applications, e.g., high-definition television and video on demand, and to provide sufficient capacity as backhauls of next-generation IEEE 802.11n wireless LANs with a throughput of 100 Mb/s or higher per device [2]. For both EPON and GPON, standardization efforts have begun to specify symmetric or asymmetric data rates of up to 10 Gb/s [26]. Recently, the IEEE standard 802.3av for 10 Gb/s EPON was approved in September 2009. DBA algorithms for EPON, GPON, and high-speed TDM PON are compared in [24].

B. WDM PON

Different forms of WDM PONs have been actively studied as a component of NG-PON [3]. A promising practical WDM PON deployment strategy on the legacy power-splitting TDM PON infrastructure selects wavelengths at each ONU using a bandpass filter (BPF) with a small insertion loss [21]. The conventional TDM ONUs are equipped with wavelength blocking filters that pass only the legacy TDM wavelength while the WDM enhanced ONUs operate on the additional wavelengths. The MPCP can be extended to support a wide range of WDM ONU structures using the reserved bits of GATE, REPORT, and other MPCP messages. Similar WDM extensions can be designed for GPON with the reserved bits in BWmap, DBRu, and other fields of each time frame. In WDM PONs, so-called colorless (i.e., wavelength-independent) ONUs should be deployed such that only a single type of WDM ONU is required, thereby greatly simplifying inventory, maintenance, and installation [21]. A promising approach toward realizing low-cost colorless ONUs is to use a reflective semiconductor optical amplifier (RSOA) at the ONU to perform remote modulation, amplification, and reflection of an optical seed signal sent by the OLT. The optical seed signal can be either (i) a modulated signal carrying downstream data, or (ii) an unmodulated *empty carrier*. In the former case, the ONU reuses the modulated carrier by means of *remodulation* techniques, e.g., FSK for downstream and OOK for upstream [3].

C. Long-reach PON

Long-reach PONs increase the range and split ratio of conventional TDM and WDM PONs significantly [27]. State-of-the-art long-reach PONs are able to have a total length of 100 km potentially supporting 17 power-splitting TDM PONs, each operating at a different pair of upstream and downstream wavelength channels and serving up to 256 colorless ONUs, translating into a total of 4352 colorless ONUs [28]. Importantly, such long-reach PON technologies allow for the integration of optical access and metro networks, i.e., broaden the functionality of PONs. This broadened PON functionality offers major cost savings by reducing the number of required optical-electrical-optical (OEO) conversions, at the expense of optical amplifiers required to compensate for propagation and splitting losses [27].

D. Migration Toward Integrated Access-Metro Networks

To provide backward compatibility with legacy infrastructure, current TDM PONs are expected to evolve toward NG-PONs in a pay-as-you-grow manner [29]. Fig. 1 depicts a tree network architecture for an evolutionary upgrade from legacy TDM ONUs to WDM ONUs and long-reach ONUs (LR ONUs), which was originally proposed, but not formally analyzed, in [30]. We briefly review this tree architecture here and incorporate it as a subnetwork for building an NG-PON in our original capacity and delay analysis. The OLT deploys one $\mathrm{TX}_{\mathrm{TDM}}$ and one $\mathrm{RX}_{\mathrm{TDM}}$ to send and receive control and data on the legacy downstream and upstream wavelength channels $\lambda_{\mathrm{TDM}}^{\mathrm{down}}$ and $\lambda_{\mathrm{TDM}}^{\mathrm{up}}$, respectively. In addition, the OLT may deploy W fixed-tuned transmitters and W fixed-tuned receivers, $W \geq 0$, which operate on W different wavelength channels $\lambda_1, \ldots, \lambda_W$. The two wavelength channels $\lambda_{\mathrm{TDM}}^{\mathrm{down}}$ and $\lambda_{\mathrm{TDM}}^{\mathrm{up}}$ together with the W wavelength channels make up the waveband Λ_{OLT}, whose $2 + W$ wavelengths allow for direct optical communication between OLT and ONUs. The OLT may use additional L fixed-tuned transmitters $\mathrm{TX}_{\mathrm{LR}}$ (but no additional receivers), $L \geq 0$, operating on L separate wavelength channels $\lambda_{W+1}, \ldots, \lambda_{W+L}$, which make up the waveband Λ_{AWG}.

In the downstream direction, the two wavebands Λ_{OLT} and Λ_{AWG} are combined via a multiplexer (MUX) and guided by the circulator toward the coupler which equally distributes both wavebands among all N ONUs. In the upstream direction, the WDM coupler in front of the OLT is used to separate the two wavebands from each other. The waveband Λ_{OLT} is forwarded to the circulator which guides it onwards to the demultiplexer (DEMUX) which in turn guides each wavelength channel to a different fixed-tuned receiver. In contrast, the waveband Λ_{AWG} optically bypasses the OLT, possibly amplified, on its way to an Arrayed-Waveguide Grating (AWG) [31] which enables long-reach optical communication between ONUs and a remote Central Office (CO) as well as single-hop optical communication from ONUs in one NG-PON to ONUs in another NG-PON.

As shown in Fig. 1, three different types of ONU architecture are considered:

a) TDM ONU: The TDM ONU is identical to an ONU of a conventional TDM EPON/GPON tree network, whereby some TDM ONUs may be upgraded to high-speed TDM ONUs. It is equipped with a single fixed-tuned transmitter $\mathrm{TX}_{\mathrm{TDM}}$ operating on the upstream wavelength channel $\lambda_{\mathrm{TDM}}^{\mathrm{up}}$ and a single fixed-tuned receiver $\mathrm{RX}_{\mathrm{TDM}}$ on the downstream wavelength channel $\lambda_{\mathrm{TDM}}^{\mathrm{down}}$. Each wavelength channel is used to send both data and control.

b) WDM ONU: The WDM ONU additionally can send and receive data on any wavelength channel $\lambda_1, \ldots, \lambda_W$ of waveband Λ_{OLT} using an extra BPF and RSOA. The BPF can be tuned to any wavelength λ_i, $i = 1, \ldots, W$, and blocks all other wavelengths. The wavelength λ_i passing the BPF is forwarded to the RSOA, which operates in either the (i) empty carrier or (ii) remodulation mode (see Section IV-B).

c) LR ONU: The LR ONU builds on the WDM ONU by having a second RSOA whose associated BPF is tunable over the wavelengths $\lambda_{W+1}, \ldots, \lambda_{W+L}$. As a result, the LR ONU can send and receive data also on any wavelength channel of waveband Λ_{AWG}, which optically bypasses the OLT. Apart from the two pairs of BPF and RSOA, the LR ONU deploys an additional multiwavelength receiver $\mathrm{RX}_{\mathrm{LR}}$ that is able to simultaneously receive data on all L wavelength channels of waveband Λ_{AWG} coming from the AWG.

The tree network in Fig. 1 accommodates N_T TDM ONUs, N_W WDM ONUs, and N_L LR ONUs, whereby $0 \leq N_T, N_W, N_L \leq N$, $N_T + N_W + N_L = N$, and N denotes the total number of ONUs.

As illustrated in Fig. 2, the OLTs of $P - 1$, $P > 2$, NG-PON access networks (shown in Fig. 1) and the remote CO in a metro area may be interconnected with any combination of (i) a bidirectional metro ring network, e.g., Gigabit Ethernet or RPR, with N_r ring nodes, (ii) a wavelength-broadcasting $P \times P$ passive star coupler (PSC) with Λ_{PSC} wavelength

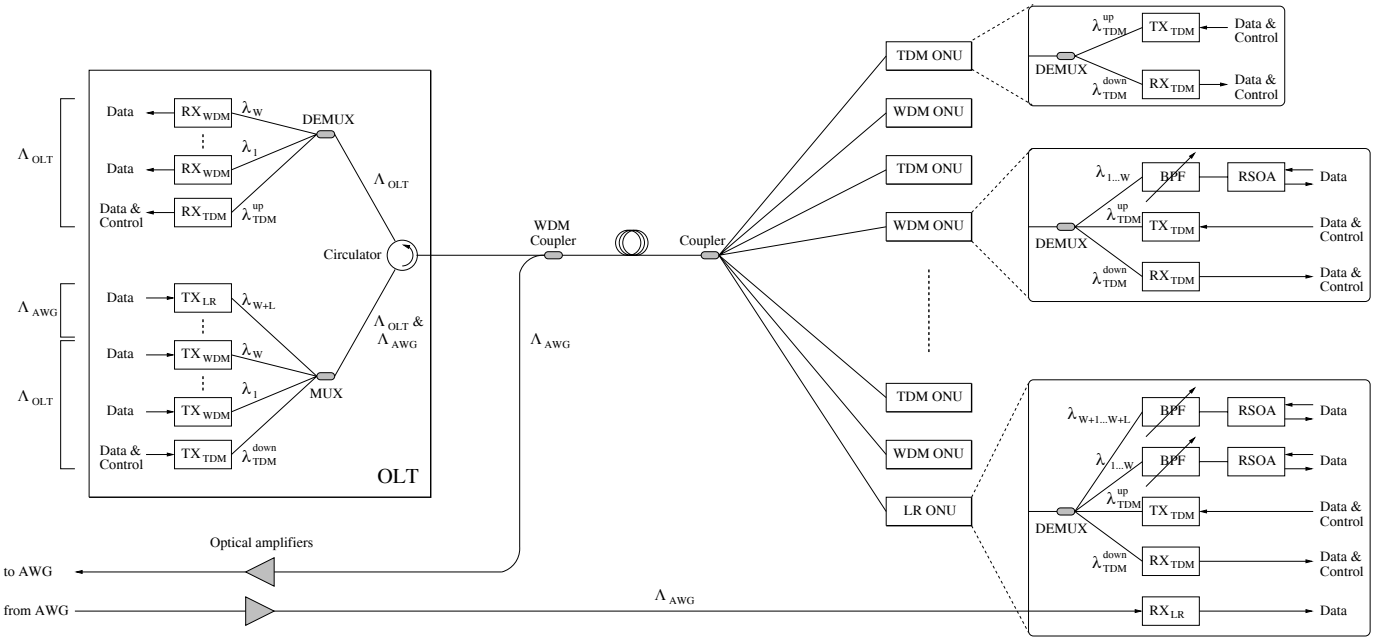

Fig. 1. Evolutionary upgrade of legacy TDM ONUs to WDM ONUs and long-reach ONUs (LR ONUs) and their coexistence on the same NG-PON fiber infrastructure.

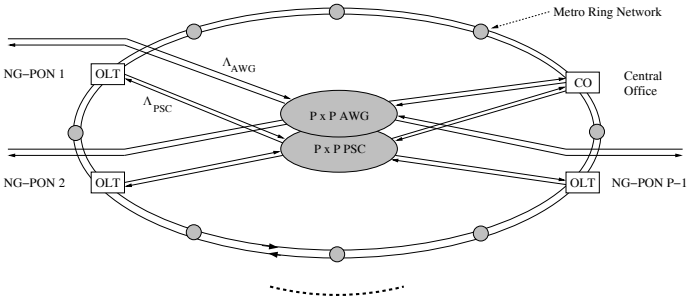

Fig. 2. Integration of NG-PONs and remote central office using the AWG as a wavelength router and a bidirectional metro ring and star subnetwork for enhanced resilience.

channels, comprising P data wavelength channels (one assigned to each OLT and CO) and one control wavelength for conducting a reservation based medium access control, and (iii) an AWG employed as a $P \times P$ wavelength router. The AWG provides any-to-any optical single-hop connections among the $P-1$ NG-PONs and the CO, i.e., integrates access and metro networks into one single-hop optical network, while allowing for spatial reuse of all Λ_{AWG} wavelengths at each AWG port [32]. Using two or more of these interconnections options in parallel enhances network resilience. Due to space constraints we refer to [33] for details on the integration network architecture in Fig. 2, and note that [33] did not conduct a detailed throughput-delay analysis.

V. Capacity and Delay Analysis

A. Overview

In this section we analyze the constraints on the capacity, i.e., the maximum (long-run) mean packet throughput, and the mean packet delay (from packet generation until complete delivery of packet to destination) of the subnetworks of the NG-PONs presented in Section IV-D. In particular, we analyze the capacity and delay of the TDM up/downstream channels and the WDM up/downstream channels in the tree network in Fig. 1 as well as the ring, PSC, and AWG subnetworks in Fig 2. This comprehensive analysis allows for the capacity and delay characterization of a wide range of NG-PONs built from the individual subnetworks through (i) the minimum of the capacities of the employed subnetworks, and (ii) appropriate weighing of the delays of the individual subnetworks.

B. Network Model

Let C_T, C_W, C_A, C_P, and C_R denote the transmission capacities [in bits per second] of one TDM, WDM, AWG, PSC, and ring channel, respectively. The defined transmission capacities account for all per-Ethernet frame overheads, such as preamble and interpacket gap. We neglect the per-cycle overheads, such as schedule compute time in the OLT, and per-ONU overheads, such as guard time. These overheads, which have been extensively studied in [23], [24], become negligible for moderate to large traffic loads and correspondingly long cycles and per-ONU transmission windows. Our analysis considers the full detail of the polling-based medium access control and thus uncovers the fundamental underlying performance characteristics due to the different polling timing structures, i.e., variable-length cycles in EPON and fixed-length frames in GPON.

We denote $\mathcal{N}$ for the set of nodes that act as (payload) traffic sources and destinations and $\eta = |\mathcal{N}|$ for the number of nodes in $\mathcal{N}$. Specifically, we consider $\mathcal{N}$ to contain H COs, N_r ring nodes, and all $(P-H)\cdot N$ ONUs in the tree subnetworks. We denote $\mathcal{C}_k$ for the set of all ONUs that are connected to OLT k. Additionally, we denote $\mathcal{C}_k^T$ for the set of TDM ONUs connected to OLT k, and analogously $\mathcal{C}_k^W$ and $\mathcal{C}_k^L$ for the sets

of WDM and LR ONUs, respectively.

We define the traffic matrix $T = (T(i,j)),\ i,j \in \mathcal{N}$, where $T(i,j)$ represents the number of packets per second that are generated at node i and destined to node j (whereby $T(i,j) = 0$ for $i = j$). For the stability analysis we assume that the traffic generation is ergodic and stationary. Importantly, the traffic matrix $T = (T(i,j)),\ i,j \in \mathcal{N}$, accounts only for the traffic that is *not* sent over the AWG, the AWG is analyzed separately as detailed shortly. For each node $i,\ i \in \mathcal{N}$, we denote

$$\sigma(i) := \sum_{l \in \mathcal{N}} T(i,l), \tag{1}$$

for the total packet traffic generation rate [in packets/second]. We denote $\bar{L}$ and σ_L^2 for the mean and variance of the packet length (including all per-Ethernet frame overheads).

1) Traffic Rates in Ring/PSC Star Subnetwork: First let us consider the traffic that is eventually sent over the ring/PSC star subnetwork. The traffic that arrives from the ONUs at OLT k (over the conventional TDM or WDM channels) and is destined to another OLT $l,\ l \neq k$, enters the ring/PSC star subnetwork. Hence, the packet rate of the ring/PSC star traffic between the two OLTs k and $l,\ k \neq l$, is given by

$$\sigma(k,l) := \sum_{i \in \mathcal{C}_k,\ j \in \mathcal{C}_l} T(i,j). \tag{2}$$

Note that traffic from an ONU i to another ONU $j,\ j \neq i$, attached to the same OLT k, i.e., with $i,j \in \mathcal{C}_k$, does not enter the ring/PSC star subnetwork. The packet traffic rates between (k,l) pairs of ring nodes, COs, and OLTs are defined analogously to (2). The defined $\sigma(k,l)$ [in packets/second] completely determine the packet traffic rates in the ring/PSC star subnetwork.

2) Traffic Rates in AWG Star Subnetwork: In addition to traffic that is sent over the tree and ring/PSC star subnetwork, an LR ONU or CO may generate traffic that is eligible for transmission over the AWG. We suppose that an LR ONU/CO that generates a packet for another LR ONU/CO that *can* be reached via the AWG, i.e., there exists a link over the AWG between the considered LR ONUs/COs, *will* send that packet over the AWG, and *not* over the tree and ring/PSC star subnetworks. Formally, we let $c(k,l)$ denote the number of wavelength channels over the AWG between OLT k and OLT l. We denote $T^A(i,j)$ for the packet traffic rate in number of generated packets per second from LR ONU/CO i to LR ONU/CO j. If $c(k,l) = 0$, i.e., if there is no link over the AWG from LR ONU $i \in \mathcal{C}_k^L$ to LR ONU $j \in \mathcal{C}_l^L$, then $T^A(i,j) = 0$. For LR ONU/CO i, we define

$$\sigma^A(i) := \sum_{l \in \mathcal{N}} T^A(i,l), \tag{3}$$

as the total packet generation rate [in packets/second] of traffic transmitted over the AWG. Note that an LR ONU/CO i may also generate traffic that is transmitted over the tree and ring/PSC star subnetwork; specifically, for ring node, TDM ONU, and WDM ONU destinations, or for LR ONU/hotspot destinations not reachable from LR ONU/CO i via the AWG. This "non-AWG" traffic is accounted for in $\sigma(i)$ given by (1).

C. Capacity Analysis

1) Capacity of Tree Subnetwork:

a) Upstream Capacity: Each ONU must not generate more traffic than it can send in the long term average, i.e.,

$$\bar{L} \cdot \sigma(i) < \begin{cases} C_T & i \in \mathcal{C}_k^T \\ C_W + C_T & i \in \mathcal{C}_k^W \cup \mathcal{C}_k^L. \end{cases} \tag{4}$$

Similarly, for each LR ONU $\bar{L} \cdot \sigma^A(i) < C_A$. The TDM ONUs at a given OLT k must not transmit more than C_T upstream, i.e.,

$$\lambda^{T,u,k} := \sum_{i \in \mathcal{C}_k^T} \bar{L} \cdot \sigma(i) < C_T. \tag{5}$$

The WDM and LR ONUs send over the WDM channels and use the remaining bandwidth of the upstream TDM channel:

$$\lambda^{W,u,k} := \sum_{i \in \mathcal{C}_k^W \cup \mathcal{C}_k^L} \bar{L} \cdot \sigma(i) < WC_W + C_T - \lambda^{T,u,k}. \tag{6}$$

We note that empty carrier upstream transmission, which requires switching between upstream and downstream transmissions, does not reduce the capacity since the finite switchover time becomes negligible for heavy traffic.

b) Downstream Capacity: The traffic arriving for the TDM ONUs has to satisfy

$$\lambda^{T,d,k} := \sum_{j \in \mathcal{C}_k^T} \sum_{l \in \mathcal{N}} \bar{L} \cdot T(l,j) < C_T. \tag{7}$$

With remodulation for the WDM upstream transmission, upstream and downstream transmissions are independent. The restriction for upstream traffic is (6) and for the downstream,

$$\lambda^{W,d,k} := \sum_{j \in \mathcal{C}_k^W \cup \mathcal{C}_k^L} \sum_{l \in \mathcal{N}} \bar{L} \cdot T(l,j) < WC_W + C_T - \lambda^{T,d,k}. \tag{8}$$

With the empty carrier approach, we can only use a WDM channel for either upstream or downstream transmission, resulting in the additional restriction

$$\lambda^{W,d,k} + \lambda^{T,d,k} + \lambda^{T,u,k} + \lambda^{W,u,k} < C_T + WC_W. \tag{9}$$

2) Capacity of the Ring/PSC Star Subnetwork: The $\sigma(k,l)$ defined in Section V-B1 correspond to the respective $\sigma(i,j)$ in [34]. Further, we can introduce and calculate the analogous probabilities to $p_{k,l}(e)$ and $p_{k,l}(m,n)$ in [34]. Specifically, for our context, we introduce the probabilities $p_{i,j}(k,l)$ that traffic from a node $i \in \mathcal{N}$ to a node $j \in \mathcal{N}$ traverses the network link (k,l). These probabilities can be precomputed for given traffic matrices T and T^A for any pair of nodes in the network. The stability condition of the ring subnet is then given by (8) in [34].

Regarding the PSC, all traffic that is generated for destination OLT l has to queue up in a *virtual queue* that is calculated by all OLTs. The total rate of traffic $\lambda^P(l)$ [in bit/second] from the PSC into OLT l must satisfy

$$\lambda^P(l) := \sum_{\text{OLT } k,\ k \neq l} \sum_{i,j \in \mathcal{N}} p_{i,j}(k,l) \cdot \bar{L} \cdot \sigma(i,j) < C_P. \tag{10}$$

3) Capacity of the AWG: In the considered NG-PON setting, the potential for collisions exists in the AWG star subnetwork only at the AWG input ports (local scheduling by the OLT avoids actual collisions). For the capacity analysis, it suffices therefore to focus on the wavelength channels running from the LR ONUs at a given OLT to the corresponding AWG input port. The traffic generated by the LR ONUs of OLT k destined toward LR ONUs at OLT l must be accommodated on the $c(k,l),\ c(k,l) \geq 0$, wavelength channels that are routed from the AWG input port of OLT k to the AWG output port leading to OLT l. The total average rate of traffic $\lambda^A(k,l)$ transmitted from OLT k over the AWG to OLT l must satisfy:

$$\lambda^A(k,l) := \sum_{i \in \mathcal{C}_k^L,\ j \in \mathcal{C}_l^L} \bar{L} \cdot T^A(i,j) < C_A \cdot c(k,l). \quad (11)$$

4) Summary of Capacity Analysis: We summarize the capacity analysis by noting that for given traffic patterns $T(i,l)$ and $T^A(i,l)$ it is relatively straightforward to obtain from the capacity constraints in Sections V-C1–V-C3 bounds on the mean aggregate network throughput. In particular, we denote

$$r_T = \bar{L} \sum_{i \in \mathcal{N}} \left[\sigma(i) + \sigma^A(i)\right] \quad (12)$$

as the total generated traffic [in bit/second], which is equivalent to the mean aggregate throughput of the network. Each capacity constraint results in an upper bound on r_T. The tightest bound identifies the network bottleneck limiting the mean aggregate throughput.

D. Delay Analysis

We denote τ_T, τ_P, and τ_A [in seconds] for the one-way propagation delay over the tree network, as well as the PSC and AWG star subnetworks, respectively. We require that the traffic that is generated at node i and destined to node j is Poisson with packet generation rate $T(i,j)$ [packets/second] and independent of the traffic for all other combinations i', j'. For each traffic rate λ [bit/second] of Section V-C, we define a corresponding (relative) load ρ by dividing λ by the respective transmission capacity C [bit/second]. We denote

$$\Phi(\rho) := \frac{\rho\left(\frac{\sigma_L^2}{\bar{L}} + \bar{L}\right)}{2C(1-\rho)} \quad (13)$$

for the corresponding mean queuing delay in an M/G/1 queue [35].

1) Delay on the Up/Downstream EPON TDM channels: The long run average traffic rate on the downstream TDM channel from OLT k is $\lambda^{T,d,k}$ given in (7), resulting in a load $\rho^{T,d,k} = \lambda^{T,d,k}/C_T$. Thus, an initial estimate of the queueing delay of a packet prior to transmission on the downstream TDM channel is given by $\Phi(\rho^{T,d,k})$. This delay does not consider that this traffic may already have traversed adjacent ring nodes and/or other OLTs $l,\ l \neq k$, (via the PSC) if the considered EPON is part of a metro network (Fig. 2). Applying the method of Bux and Schlatter [36] to our setting, we compensate for the queueing delay at the preceding nodes by subtracting a correction term $B^{T,d,k}$ from the queueing delay $\Phi(\rho^{T,d,k})$. Following [36], the correction term $B^{T,d,k}$ is the sum of the queueing delays for the individual traffic streams that flow into OLT k from adjacent nodes *and* leave over the arc of interest, namely the downstream TDM channel. In particular,

$$B^{T,d,k} = \sum_{\text{ring node } l \text{ adjacent to OLT } k} \Phi(\rho^{l,R,T,k}) + \sum_{\text{OLT } l} \Phi(\rho^{l,P,T,k}), \quad (14)$$

with $\rho^{l,R,T,k}$ denoting the load due to traffic flowing from the adjacent ring nodes l over the ring to reach one of the TDM ONUs at OLT k and $\rho^{l,P,T,k}$ denoting the load from an OLT $l,\ l \neq k$, over the PSC to a TDM ONU at OLT k. Adding the average transmission delay $\bar{L}/C_T$ and the downstream propagation delay τ_T we obtain the total delay

$$D^{T,d,k,E} = \Phi\left(\rho^{T,d,k}\right) + \tau_T + \frac{\bar{L}}{C_T} - B^{T,d,k}. \quad (15)$$

The upstream data transmissions experience the following delay components due to the reporting and granting procedure. First, the mean delay from packet generation until transmission of the corresponding report is the mean residual cycle length of the upstream TDM channel, which is approximately τ_T. Second, the upstream propagation of the report and downstream propagation of the grant add the round trip propagation delay $2\tau_T$. Third, the queueing delay for the grant prior to its transmission on the downstream TDM channel is $\Phi(\rho^{T,d,k})$ without priority for grants, and $\rho^{T,d,k}\bar{L}/(2C_T)$ with priority for the grant messages (considered in the following). Adding packet queueing, transmission, and propagation delays gives

$$D^{T,u,k,E} = 4\tau_T + \Phi(\rho^{T,u,k}) + \frac{\bar{L}}{C_T} + \frac{\rho^{T,d,k}\bar{L}}{2C_T}. \quad (16)$$

2) Delay on the EPON WDM Channels:

a) Remodulated Carrier for Upstream Transmission: The WDM channels can be continuously used for downstream and upstream transmission. The traffic rate for the downstream WDM channels is given by $\lambda^{W,d,k}$ (8). The queueing delay can be approximated by the queueing delay in an M/G/W queueing system. Since there is no explicit delay formula for such a system, we further approximate by considering an M/G/1 queue with a server with transmission rate WC_W, i.e., we consider an M/G/1 queue with load $\rho^{W,d,k} = \lambda^{W,d,k}/(WC_W)$,

$$D^{W,d,k,E} \approx \Phi\left(\frac{\lambda^{W,d,k}}{WC_W}\right) + \tau_T + \frac{\bar{L}}{C_T} - B^{W,d,k}, \quad (17)$$

where $B^{W,d,k}$ is defined analogously to (14). For the upstream direction we obtain analogously to (16): $D^{W,u,k,E} \approx 4\tau_T + \Phi\left(\frac{\lambda^{W,u,k}}{WC_W}\right) + \frac{\bar{L}}{C_W} + \frac{\rho^{T,d,k}\bar{L}}{2C_W}$.

b) Empty Carrier for Upstream Data Transmission: With switching between upstream and downstream transmissions, the combined upstream and downstream traffic has to be accommodated on the WDM channels, resulting in the load $\rho^{W,k} = \frac{\lambda^{W,d,k}+\lambda^{W,u,k}}{WC_W}$ and a queueing delay of approximately $\Phi(\rho^{W,k})$. As detailed in [37] the delay contribution due to switchovers can be approximated through a superposition of Poisson processes and incorporated as a shift in the packet length distribution to mean $\bar{L}+p_{s,k}C_W\tau_T$ and second moment $\sigma_L^2+2\bar{L}p_{s,k}C_W\tau_T+p_{s,k}(C_W\tau_T)^2$. Using this modified packet

length distribution, we obtain the delay on the WDM channels as

$$D^{W,d,k} = \Phi(\rho^{W,k}) + \tau_T + \frac{\bar{L}}{C_T} - B^{W,d,k}. \quad (18)$$

The upstream traffic experiences additional delay components due the reporting and granting procedure analogous to the analysis leading to (16). Thus, $D^{W,u,k} := D^{W,d,k} + 3\tau_T + \frac{\rho^{T,d,k}\bar{L}}{2C_T}$.

3) Delay on GPON: Let δ denote the frame duration of 125 μs of the GPON. A packet generated at an ONU has to wait on average $\delta/2$ for the beginning of the next frame in which it will be reported in a DBRu field. This next frame has a duration (transmission delay) of δ and takes τ_T to propagate to the OLT. Once arrived at the OLT, the bandwidth report is processed and the grant for the packet's transmission is included in the BWmap of the next downstream frame. Even with negligible processing time at the OLT, there is a delay of up to δ until the beginning of the next downstream frame. More specifically, let ω, $0 \leq \omega < \delta$, [in seconds] denote the offset between the upstream and downstream channels defined as follows. At the instant when a new slot starts on the upstream channel, ω seconds have passed of the current downstream channel slot, i.e., for $\omega = 0$, the slots on the upstream and downstream channels are aligned. Then, the time until the beginning of the downstream frame containing the BWmap of the considered packet is $\gamma_1 = \left(1 - \left(\frac{\tau_T-\omega}{\delta} - \left\lfloor\frac{\tau_T-\omega}{\delta}\right\rfloor\right)\right)\delta$.

The downstream frame has a transmission delay of δ and propagation delay of τ_T. The packet has to wait for $\gamma_2 = \left(1 - \left(\frac{\tau_T+\omega}{\delta} - \left\lfloor\frac{\tau_T+\omega}{\delta}\right\rfloor\right)\right)\delta$ until the beginning of the next upstream frame before it can possibly be transmitted. Thus, it takes overall on average $5\delta/2+\tau_T+\gamma_1+\tau_T+\gamma_2$ from the instant the packet is generated to the instant the packet becomes eligible for upstream transmission. And then, the packet is put into a general queue for the upstream channel. In terms of the mean packet delay, this channel can be modeled as an M/G/1 queue (noting that the specific scheduling discipline does not affect the overall mean packet delay in the GPON, as long as the channel is operated in work conserving manner, i.e., is not left idle while packets are queued), with corresponding delay $\Phi(\rho^{T,u,k})$. Finally, the packet experiences the transmission delay $\bar{L}/C_T$ and propagation delay τ_T. Overall, the mean delay for the TDM upstream channel is

$$D^{T,u,k,G} = \frac{5\delta}{2} + \gamma_1 + \gamma_2 + \Phi(\rho^{T,u,k}) + 3\tau_T + \frac{\bar{L}}{C_T}. \quad (19)$$

The WDM upstream channels experience the analogous delays for the report-grant cycle but carry the load $\lambda^{W,u,k}/(WC_W)$, i.e., we obtain $D^{W,u,k,G}$ by replacing $\Phi(\rho^{T,u,k})$ by $\Phi(\lambda^{W,u,k}/(WC_W))$ in (19).

The TDM downstream channel is analyzed analogously giving

$$D^{T,d,k,G} = \frac{\delta}{2} + \Phi\left(\rho^{T,d,k}\right) + \tau_T + \frac{\bar{L}}{C_T^k} - B^{T,d,k}. \quad (20)$$

The delay for the downstream WDM channels is obtained by replacing $\Phi\left(\rho^{T,d,k}\right)$ by $\Phi\left(\frac{\lambda^{W,d,k}}{WC_W}\right)$ in (20).

4) Delay in the Ring/PSC Star Subnetwork: With τ_P^f denoting the frame duration [in seconds] on the PSC, a newly arrived packet at the OLT waits on average $\tau_P^f/2$ before its control packet can be sent. The control packet experiences a propagation delay of τ_P. Once the control packet is received, the packet enters the virtual queue for the destination OLT. This queue experiences a load of $\rho^{P,l} = \lambda^P(l)/C_P$ with $\lambda^P(l)$ given in (10). Adding in the data packet transmission and propagation delays, we obtain

$$D^P(l) = \frac{\tau_P^f}{2} + 2\tau_P + \Phi(\rho^{P,l}) + \frac{\bar{L}}{C_P} - B^{P,l}, \quad (21)$$

with the correction term $B^{P,l} = \sum_{\text{OLT } k}\left[\sum_m \Phi(\rho^{R,P,m,k,l}) + \Phi(\rho^{T,P,k,l}) + \Phi(\rho^{W,P,k,l})\right]$ whereby the inner sum is over the ring nodes m adjacent to OLT k; further, $\rho^{R,P,m,k,l}$ denotes the traffic that originates at ring node m and flows over the PSC from OLT k to OLT l, and $\rho^{T,P,k,l}$ and $\rho^{W,P,k,l}$ denote the analogous traffic loads for the TDM and WDM channels (see [37] for details).

The packet delay in the ring/PSC star subnetwork $D_{ij}^{R,P}$ from an OLT/CO i to another OLT/CO (or a destination ring node) j is given by Eqn. (22) in [34] with the last two sums replaced by $D_{ij}^P = \sum_{k,l} p_{ij}(k,l)D^P(l)$. The packet delay from a ring node to a CO/hotspot (or a destination ring node) is given by Eqn. (21) in [34] with the last sum replaced by D_{ij}^P.

5) Delay in AWG Star Subnetwork: The packet delay in the AWG star subnetwork is approximately

$$D^A(k,l) = 3\tau_T + \frac{\rho^{T,d,k}\bar{L}}{2C_T} + \Phi(\rho^A(k,l)) + \tau_A + \frac{\bar{L}}{C_A}, \quad (22)$$

where the first two terms are due to the report-grant cycle using the upstream TDM channel. Averaging, using the $\lambda^A(k,l)$ (11) as weights, gives the average packet delay D^A on the AWG star subnetwork:

$$D^A = \sum_{\text{OLT } k,\, l} D^A(k,l) \cdot \frac{\lambda^A(k,l)}{\sum_{\text{OLT } k',\, l'} \lambda^A(k',l')}. \quad (23)$$

E. Overall Delay

We obtain the overall average packet delay by weighing the delays $D(i,j)$ of the different paths according to their packet traffic rates $T(i,j)$. First, for traffic transmitted over the ring/PSC star subnetwork $D^{R,P} = \sum_{i,j} D(i,j)\,\frac{T(i,j)}{\sum_{i',j'} T(i',j')}$. For instance, $D(i,j) = D_{il}^{R,P} + D^{T,d,l}$ for traffic from ring node/CO i to TDM ONU j at OLT l (resp. $D^{W,d,l}$ for traffic to WDM or LR ONU at OLT l). Overall, we obtain the mean packet delay as

$$D = D^{R,P}\frac{\sum_{i,j} T(i,j)}{\sum_{i,j} T(i,j) + \sum_{\text{LR ONUs } i,j} T^A(i,j)} + D^A\frac{\sum_{\text{LR ONUs } i,j} T^A(i,j)}{\sum_{i,j} T(i,j) + \sum_{\text{LR ONUs } i,j} T^A(i,j)}. \quad (24)$$

VI. Numerical and Simulation Results

This section presents numerical results on the throughput-delay performance, first for isolated PONs and then for integrated access-metro networks, obtained from our analysis

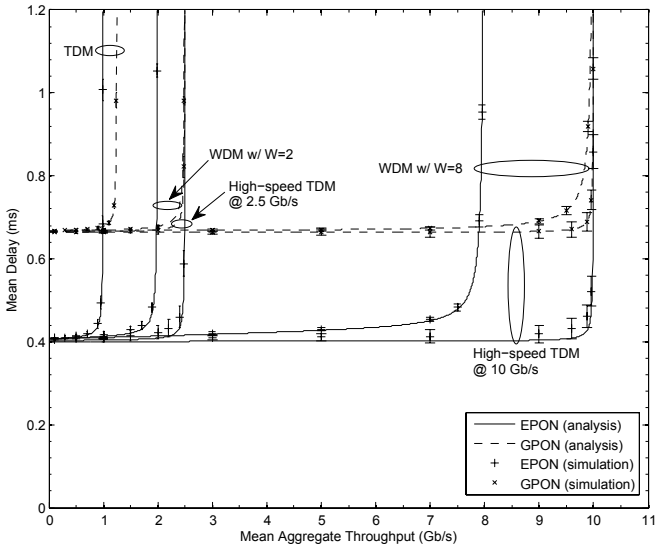

Fig. 3. Mean delay D on upstream TDM/WDM channels of high-speed TDM and WDM EPON/GPON vs. mean aggregate throughput r_T for $N_T = 32$ TDM ONUs and $N_W = 32$ WDM ONUs, respectively.

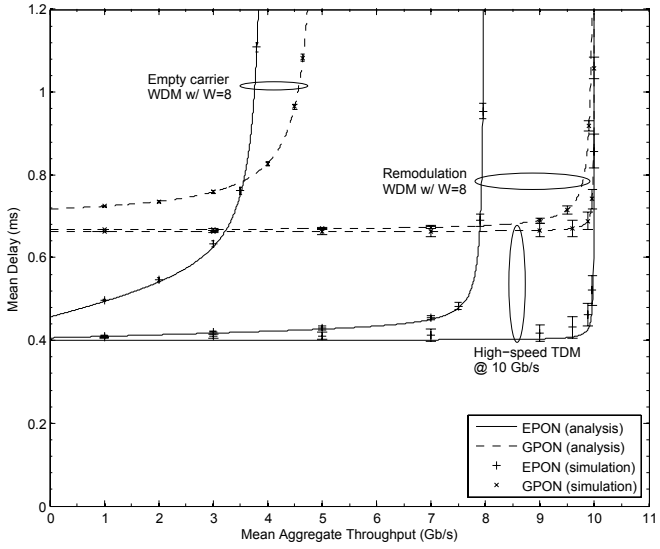

Fig. 4. Mean delay D vs. mean aggregate throughput r_T of WDM EPON/GPON using remodulation and empty carrier.

and extensive verifying simulations with 95% confidence intervals. The propagation speed is set to $2 \cdot 10^8$ m/s. We first consider uniform traffic where each ONU generates the same amount of packet traffic with a packet size randomly uniformly distributed over $[64, 1518]$ bytes. In the context of an isolated PON, a packet generated by a given ONU is destined to any of the other $N-1$ ONUs of the same PON with equal probability $1/(N-1)$.

A. Isolated PONs

Fig. 3 compares the mean delay D on the upstream TDM/WDM channels of conventional TDM, high-speed TDM, and WDM EPON/GPON networks vs. the mean aggregate throughput r_T. We consider an EPON with $C_T = 1$ Gb/s and a (symmetric) GPON with $C_T = 1.25$ (and $\omega = 0$) whereby the ONUs are located at 20 km from the OLT. We consider a fixed number of $N_T = 32$ TDM ONUs and $N_W = 32$ WDM ONUs, respectively. Both high-speed TDM PONs operate at a data rate of $C_T \in \{2.5, 10\}$ Gb/s. In addition to the pair of legacy TDM wavelength channels, the WDM EPON and WDM GPON deploy $W \in \{2, 8\}$ wavelength channels via remodulation, each operating at $C_W = C_T = 1$ Gb/s and $C_W = C_T = 1.25$ Gb/s, respectively. We observe that the EPON achieves significantly lower delays than the GPON at small to medium traffic loads. This EPON advantage is due to its underlying variable-length polling cycle compared to the fixed length framing structure of the GPON. We further observe that analysis and simulation results match very well, except that the analysis underestimates the mean EPON delay slightly at medium traffic loads.

Fig. 4 shows the 10 Gb/s high-speed TDM and WDM EPON/GPON with remodulation of Fig. 3 and compares them to a WDM EPON/GPON using the commercially available empty carrier approach [2]. The empty carrier approach suffers from a higher mean delay and a significantly lower mean aggregate throughput on the upstream TDM/WDM channels than a WDM EPON/GPON based on remodulation. This is due to the fact that in the empty carrier approach each WDM wavelength channel is used for bidirectional transmission, i.e., upstream and downstream transmissions alternate, as opposed to remodulation where upstream transmissions are not delayed by downstream transmissions.

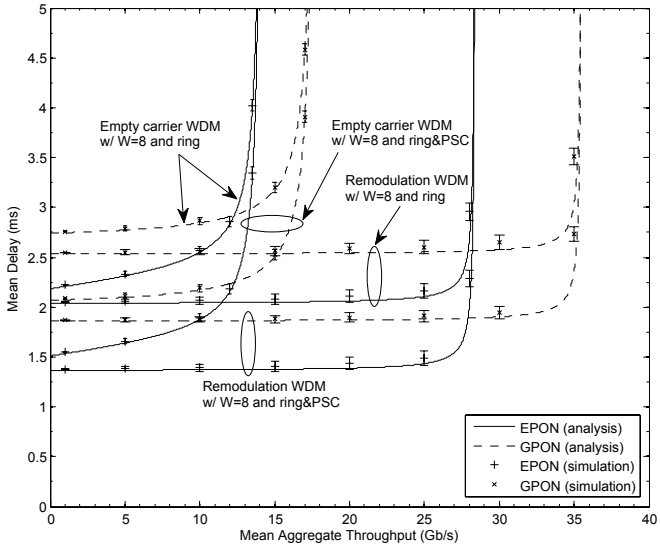

Fig. 5. Mean delay D vs. mean aggregate throughput r_T of three WDM PONs interconnected through (i) a ring, or (ii) a ring combined with a 4×4 PSC.

B. Integrated Access-Metro Networks

Next, we investigate different methods to interconnect multiple high-speed TDM/WDM PONs by means of a ring, PSC, and/or AWG. Fig. 5 depicts the mean delay vs. mean aggregate throughput of three of the aforementioned WDM EPONs/GPONs interconnected through either (i) a ring only, or (ii) a ring in conjunction with a 4×4 PSC (i.e., $P = 4$), for shortest path (minimum hop) routing. The circumference

of the bidirectional ring is set to 100 km and it comprises $N_r = 4$ equally spaced ring nodes. Both ring and PSC operate at a data rate of 10 Gb/s, i.e., $C_R = C_P = 10$ Gb/s. We consider uniform source and destination traffic originating from and going to any of the $3 \cdot 32 = 96$ WDM ONUs, $N_r = 4$ ring nodes, and $H = 1$ remote CO (see Fig. 2). Formally, for uniform source traffic, $\sigma(i) = \sigma \ \forall i \in \mathcal{N}$ and the total traffic bit rate in the network is $r_T = \eta \bar{L} \sigma$. As shown in Fig. 5, using a PSC that provides short-cut links to the ring helps decrease the mean delay considerably, but in the considered example network configuration does not lead to an increased mean aggregate throughput. (Similar observations were made for 10 Gb/s high-speed TDM PONs, not shown here due to space constraints.) In particular, for the EPON with uniform source and uniform destination traffic, both the upstream (Eqn. (6)) and the downstream WDM channel with remodulation capacity constraint (Eqn. (8)) give the bound

$$r_T < \frac{\eta(\eta-1)(W+1)C}{(\eta-1)(N_T+N_W)+\eta_{TWr}N_L} \tag{25}$$

with $\eta_{TWr} = (P-H)(N_T+N_W)+N_r$ denoting the total number of TDM/WDM ONUs and ring nodes. For the considered scenarios with $N_W = 32$ WDM ONUs (and no TDM or LR ONUs) this bound reduces to $r_T < \eta(W+1)C/N_W = 28.4$ Gbps, which is lower than the bounds imposed by the ring and PSC (not detailed here due to space constraints, see [37] for details), and hence governs the maximum mean aggregate throughput (capacity).

In the following, we study the impact of non-uniform traffic on the throughput-delay performance of NG-PONs. Let us first focus on *non-uniform source traffic*, where nodes generate different traffic rates. For now, we continue to consider uniform destination traffic. More specifically, N_m of the ONUs in each NG-PON as well as all N_r ring nodes generate traffic at a medium bit rate of $\sigma\bar{L}$. Furthermore, we introduce a source traffic non-uniformity α, $\alpha \geq 1$, and let N_l lightly loaded ONUs in each NG-PON generate traffic at a low bit rate of $\sigma\bar{L}/\alpha$, and N_h highly loaded ONUs in each NG-PON as well as the remote CO generate traffic at a high bit rate of $\alpha\sigma\bar{L}$. Note that $\alpha = 1$ denotes uniform traffic, which has been studied above.

Fig. 6 compares the mean delay vs. mean aggregate throughput performance of three WDM EPONs with $W = 8$ wavelengths in remodulation mode, each operating at 1 Gb/s, with that of three 10 Gb/s high-speed TDM EPONs, interconnected with the remote CO through a ring in conjunction with (i) a 4×4 PSC, or (ii) a 4×4 AWG using $\Lambda_{\text{AWG}} = 4$ wavelengths. The ring, PSC, and AWG operate at 10 Gb/s, i.e., $C_R = C_P = C_A = 10$ Gb/s. In each EPON, we set $N_l = 16$ and $N_m = N_h = 8$ and consider different source traffic non-uniformity $\alpha \in \{1, 2, 4\}$. In the ring&PSC configuration, there are $N_W = 32$ WDM ONUs in a given WDM EPON (resp. $N_T = 32$ ONUs in a high-speed TDM EPON). In the ring&AWG configuration, the N_h highly loaded ONUs are upgraded to LR-ONUs in each high-speed WDM EPON (and each high-speed TDM EPON which is connected with P high-speed wavelength channels to the AWG).

We observe from Fig. 6 that the ring&PSC configurations are insensitive to source traffic non-uniformities. This is because the shift in traffic generation from lightly to heavily loaded ONUs with increasing source traffic non-uniformity α does not significantly shift the portion of the total network traffic load that needs to traverse the EPON downstream WDM channels. In contrast, for the ring&AWG configurations we observe from Fig. 6 increases in the aggregate network throughput as the traffic becomes more non-uniform. With increasing α, the heavily loaded ONUs account for a larger portion of the total network traffic. Thus, the traffic portion that can be off-loaded from the EPON WDM channels to the AWG channels, namely all traffic between pairs of heavily loaded ONUs, increases with α, resulting in an increased aggregate throughput. (Similar observations were made for high-speed TDM and WDM GPONs.)

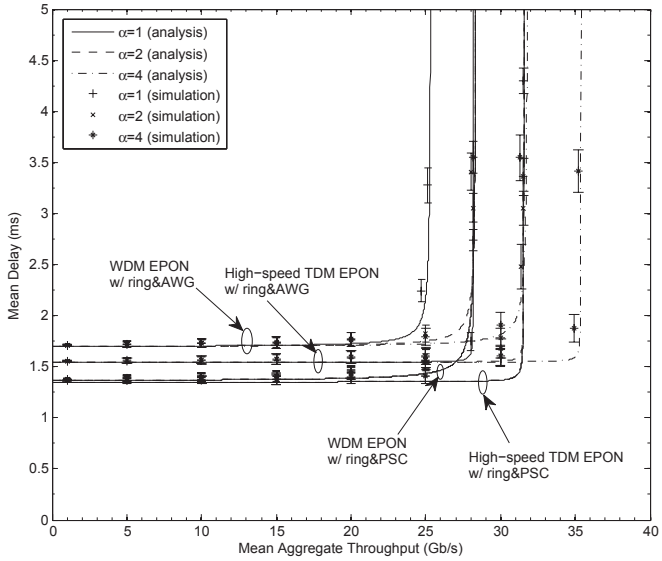

Fig. 6. Mean delay D vs. mean aggregate throughput r_T of three WDM EPONs and three high-speed TDM EPONs interconnected through (i) a ring&PSC, or (ii) a ring&AWG for different source traffic non-uniformity $\alpha \in \{1, 2, 4\}$.

Fig. 7 considers the ring&AWG configurations of the previous figure for a fixed source traffic non-uniformity $\alpha = 2$ and illustrates the impact of *non-uniform destination traffic*. Specifically, a packet generated by an LR ONU or CO is destined to another LR ONU/CO with probability $(\eta_{LH} - 1)/(\eta - 1) \leq \beta \leq 1$, whereby $\eta_{LH} = (P-1)N_h + H$ denotes the number of LR-ONUs and CO in the network. Note that in our case $\beta = (\eta_{LH}-1)/(\eta-1) = 0.24$ corresponds to uniform destination traffic. We observe from Fig. 7 that both AWG network configurations are quite sensitive to destination traffic non-uniformity. The maximum mean aggregate throughput is significantly increased as the fraction of traffic routed over the AWG increases.

VII. Conclusions

We have developed a comprehensive probabilistic analysis for evaluating the packet throughput-delay performance of next-generation PONs (NG-PONs). Our analysis accommodates both EPONs and GPONs with their various next-generation upgrades, as well as a variety of all-optical interconnections of NG-PONs. Our numerical results illustrate the

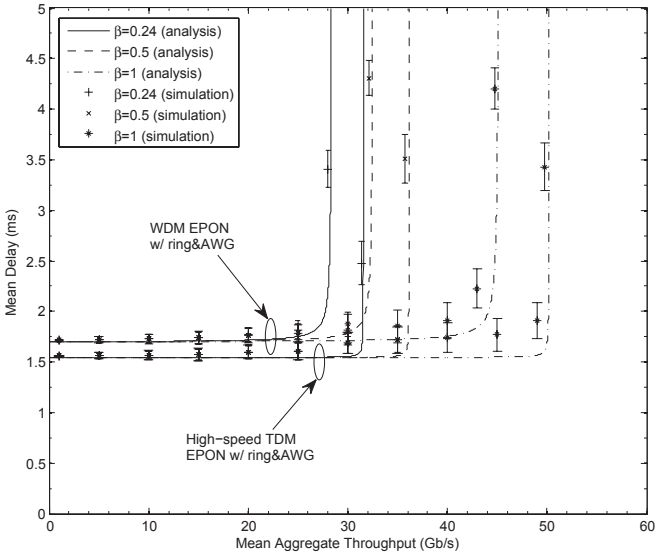

Fig. 7. Mean delay D vs. mean aggregate throughput r_T of three WDM EPONs and three high-speed TDM EPONs interconnected through a ring&AWG for $\alpha = 2$ and different destination traffic non-uniformity $\beta \in \{0.24, 0.5, 1\}$.

use of our analysis to evaluate the throughput delay performance of upgrades that increase the transmission line rates or wavelength counts. We also demonstrate the identification of network bottlenecks using our analysis.

REFERENCES

[1] M. Rad, H. A. Fathallah, and L. Rusch, "Fiber fault PON monitoring using optical coding: effects of customer geographic distribution," *IEEE Trans. Commun.*, vol. 58, no. 4, pp. 1172-1181, Apr. 2010.

[2] R. Lin, "Next generation PON in emerging networks," in *Proc. OFC/NFOEC*, Feb. 2008.

[3] K. Grobe and J.-P. Elbers, "PON in adolescence: From TDMA to WDM-PON," *IEEE Commun. Mag.*, vol. 46, no. 1, pp. 26-34, Jan. 2008.

[4] G. Kramer, B. Mukherjee, and G. Pesavento, "IPACT: a dynamic protocol for an Ethernet PON (EPON)," *IEEE Commun. Mag.*, vol. 40, no. 2, pp. 74-80, Feb. 2002.

[5] J. Zheng and H. Mouftah, "A survey of dynamic bandwidth allocation algorithms for Ethernet Passive Optical Networks," *Optical Switching Netw.*, vol. 6, no. 3, pp. 151-162, July 2009.

[6] H. Takagi, *Analysis of Polling Systems*. MIT Press, 1986.

[7] C. G. Park, D. H. Han, and K. W. Rim, "Packet delay analysis of symmetric gated polling system for DBA scheme in an EPON," *Telecommun. Syst.*, vol. 30, no. 1-3, pp. 13-34, Nov. 2005.

[8] F. Aurzada, M. Scheutzow, M. Herzog, M. Maier, and M. Reisslein, "Delay analysis of Ethernet Passive Optical Networks with gated service," *OSA J. Optical Netw.*, vol. 7, no. 1, pp. 25-41, Jan. 2008.

[9] B. Lannoo, L. Verslegers, D. Colle, M. Pickavet, M. Gagnaire, and P. Demeester, "Analytical model for the IPACT dynamic bandwidth allocation algorithm in EPONs," *OSA J. Optical Netw.*, vol. 6, no. 6, pp. 677-688, June 2007.

[10] M. T. Ngo, A. Gravey, and D. Bhadauria, "A mean value analysis approach for evaluating the performance of EPON with Gated IPACT," in *Proc. Int. Conf. Optical Netw. Design Modeling*, Mar. 2008, pp. 1-6.

[11] J. Vardakas and M. Logothetis, "Packet delay analysis for priority-based passive optical networks," in *Proc. Int. Conf. Emerging Netw. Intelligence*, Oct. 2009, pp. 103-107.

[12] W. Kwong, G.-C. Yang, and J.-G. Zhang, "2^n prime-sequence codes and coding architecture for optical code-division multiple-access," *IEEE Trans. Commun.*, vol. 44, no. 9, pp. 1152-1162, Sep. 1996.

[13] J. Vardakas, V. Vassilakis, and M. Logothetis, "Blocking analysis for priority classes in hybrid WDM-OCDMA passive optical networks," in *Proc. Fifth Advanced International Conf. Telecommun.*, 2009, pp. 389-394.

[14] W.-R. Chang, "Research and design of system architectures and communication protocols for next-generation optical networks," Ph.D. dissertation, National Cheng Kung University, Tainan, Taiwan, 2008.

[15] N. Antunes, C. Fricker, P. Roberts, and J. Roberts, "Traffic capacity of large WDM passive optical networks," in *Proc. Int. Teletraffic Congress*, Sep. 2010.

[16] F. Aurzada, M. Scheutzow, M. Reisslein, and M. Maier, "Towards a fundamental understanding of the stability and delay of offline WDM EPONs," *IEEE/OSA J. Optical Commun. Netw.*, vol. 2, no. 1, pp. 51-66, Jan. 2010.

[17] M. A. Marsan, E. Leonardi, M. Meo, and F. Neri, "Modeling slotted WDM rings with discrete-time Markovian models," *Comput. Netw.*, vol. 32, no. 5, pp. 599-615, May 2000.

[18] I. Rubin and H.-K. H. Hua, "Synthesis and throughput behavior of WDM meshed-ring networks under nonuniform traffic loading," *IEEE/OSA J. Lightwave Technol.*, vol. 15, no. 8, pp. 1513-1521, Aug. 1997.

[19] A. Girard, *FTTx PON Technology and Testing*. EXFO Electro-Optical Eng. Inc., 2005.

[20] M. D. Vaughn, D. Kozichek, D. Meis, A. Boskovic, and R. Wanger, "Value of reach-and-split ratio increase in FTTH access networks," *IEEE/OSA J. Lightwave Technol.*, vol. 22, no. 11, pp. 2617-2622, Nov. 2004.

[21] F. Effenberger, D. Clearly, O. Haran, G. Kramer, R. D. Li, M. Oron, and T. Pfeiffer, "An introduction to PON technologies," *IEEE Commun. Mag.*, vol. 45, no. 3, pp. S17-S25, Mar. 2007.

[22] J. Jiang and J. Senior, "A new efficient dynamic MAC protocol for the delivery of multiple services over GPON," *Photonic Network Commun.*, vol. 18, no. 2, pp. 227-236, Oct. 2009.

[23] M. Hajduczenia, H. J. A. da Silva, and P. P. Monteiro, "EPON versus APON and GPON: a detailed performance comparison," *OSA J. Optical Netw.*, vol. 5, no. 4, pp. 298-319, Apr. 2006.

[24] B. Skubic, J. Chen, J. Ahmed, L. Wosinska, and B. Mukherjee, "A comparison of dynamic bandwidth allocation for EPON, GPON, and next-generation TDM PON," *IEEE Commun. Mag.*, vol. 47, no. 3, pp. S40-S48, Mar. 2009.

[25] J.-I. Kani, F. Bourgart, A. Cui, A. Rafel, M. Campbell, R. Davey, and S. Rodrigues, "Next-generation PON–part I: technology roadmap and general requirements," *IEEE Commun. Mag.*, vol. 47, no. 11, pp. 43-49, Nov. 2009.

[26] F. J. Effenberger, "The XG-PON system: cost effective 10 Gb/s access," *IEEE/OSA J. Lightwave Technol.*, vol. 29, no. 4, pp. 403-409, Feb. 2011.

[27] D. Shea and J. Mitchell, "Architecture to integrate multiple PONs with long reach DWDM backhaul," *IEEE J. Sel. Areas Commun.*, vol. 27, no. 2, pp. 126-133, Feb. 2009.

[28] G. Talli and P. D. Townsend, "Hybrid DWDM-TDM long-reach PON for next-generation optical access," *IEEE/OSA J. Lightwave Technol.*, vol. 24, no. 7, pp. 2827-2834, July 2006.

[29] M. Maier, "WDM passive optical networks and beyond: the road ahead," *IEEE/OSA J. Optical Commun. Netw.*, vol. 1, no. 4, pp. 2617-2622, Sep. 2009.

[30] L. Meng, C. Assi, M. Maier, and A. Dhaini, "Resource management in STARGATE-based Ethernet passive optical networks (SG-EPONs)," *IEEE/OSA J. Optical Commun. Netw.*, vol. 1, no. 4, pp. 279-293, Sep. 2009

[31] M. Maier and M. Reisslein, "AWG based metro WDM networking," *IEEE Commun. Mag.*, vol. 42, no. 11, pp. S19-S26, Nov. 2004.

[32] M. Scheutzow, M. Maier, M. Reisslein, and A. Wolisz, "Wavelength reuse for efficient packet-switched transport in an AWG-based metro WDM network," *IEEE/OSA J. Lightwave Technol.*, vol. 21, no. 6, pp. 1435-1455, June 2003.

[33] M. Maier, M. Herzog, and M. Reisslein, "STARGATE: the next evolutionary step toward unleashing the potential of WDM EPONs," *IEEE Commun. Mag.*, vol. 45, no. 5, pp. 50-56, May 2007.

[34] M. Maier, M. Herzog, M. Scheutzow, and M. Reisslein, "PROTECTORATION: a fast and efficient multiple-failure recovery technique for resilient packet ring (RPR) using dark fiber," *IEEE/OSA J. Lightwave Technol.*, vol. 23, no. 10, pp. 2816-2838, Oct. 2005.

[35] L. Kleinrock, *Queueing Systems: Volume I: Theory*. Wiley, 1975.

[36] W. Bux and M. Schlatter, "An approximate method for the performance analysis of buffer insertion rings," *IEEE Trans. Commun.*, vol. COM-31, no. 1, pp. 50-55, Jan. 1983.

[37] F. Aurzada, M. Scheutzow, M. Reisslein, N. Ghazisaidi, and M. Maier, "Capacity and delay analysis of next-generation passive optical networks (NG-PONs)–extended version," Technical Report, Ariz. State Univ., July 2010. Available: http://mre.faculty.asu.edu/NG_PONs.pdf.

Frank Aurzada studied mathematics at the Friedrich-Schiller University, Jena, Germany and the University of York, York, U.K. He received the Dipl.-Math. and Ph.D. degrees in mathematics from the Friedrich-Schiller University in 2003 and 2006, respectively. After completing his Ph.D., he joined the DFG Research Center Matheon at Technical University Berlin, where he is currently a Postdoctoral Researcher. His research interests lie in the queueing theoretic analysis of telecommunication networks, coding theory, and limit theorems in probability theory. He is currently the head of an Independent Junior Research Group at TU Berlin.

Michael Scheutzow is a Professor in the Department of Mathematics at the Technical University Berlin, Germany. He received the Diploma in Mathematics from the Johann-Wolfgang-Goethe University Frankfurt/Main, Germany, in 1979. He received his Ph.D. in Mathematics (magna cum laude) from the University of Kaiserslautern, Germany, in 1983. He received his Habilitation in Mathematics from the University of Kaiserslautern in 1988. From 1988 through 1990 he was project leader with Tecmath GmbH, Kaiserslautern. Since 1990 he is Professor of Stochastics in the Department of Mathematics at the TU Berlin. From 1997 through 1999 he was Associate Chair of the department. He has visited the Univ. Carbondale, Ill., Rutgers Univ., Univ. of Rochester, Warwick Univ., and the MSRI at UC Berkeley.

Martin Reisslein (A96-S97-M98-SM03) is an Associate Professor in the School of Electrical, Computer, and Energy Engineering at Arizona State University (ASU), Tempe. He received the Dipl.-Ing. (FH) degree from the Fachhochschule Dieburg, Germany, in 1994, and the M.S.E. degree from the University of Pennsylvania, Philadelphia, in 1996; both in electrical engineering. He received his Ph.D. in systems engineering from the University of Pennsylvania in 1998. During the academic year 1994-1995 he visited the University of Pennsylvania as a Fulbright scholar. From July 1998 through October 2000 he was a scientist with the German National Research Center for Information Technology (GMD FOKUS), Berlin and lecturer at the Technical University Berlin. He currently serves as Associate Editor for the IEEE/ACM TRANSACTIONS ON NETWORKING and for *Computer Networks*. He maintains an extensive library of video traces for network performance evaluation, including frame size traces of MPEG-4 and H.264 encoded video, at http://trace.eas.asu.edu. His research interests are in the areas of multimedia networking, optical access networks, and engineering education.

Navid Ghazisaidi (navid.ghazisaidi@ericsson.com) is with Ericsson Inc., San Jose, CA. He received his MSc. degree in Electrical Engineering with specialization in Telecommunications (with distinction) from the Blekinge Institute of Technology (BTH), Karlskrona, Sweden in 2006, and his Ph.D. degree in Telecommunications from the University of Quebec, INRS, Montréal, Canada, in 2010. Dr. Ghazisaidi was a Research Associate with Arizona State University, Tempe, AZ, from September 2010 through November 2010. He was a Visiting Researcher at the Deutsche Telekom Laboratories (T-Labs), Berlin, Germany, and participated in the European research project ACCORDANCE (A Converged Copper-Optical-Radio OFDMA-based Access Network with high Capacity and flExibility), January 2010 through April 2010. He was a Researcher in the Computer Network (CN) group at the University of Basel, Basel, Switzerland, and participated in the European research project BIONETS (BIOlogically-inspired autonomic NETworks and Services), September 2006 through January 2007. His research interests are in the area of MAC protocol design for Fiber-Wireless (FiWi) networks.

Martin Maier (maier@ieee.org) (M03-SM08) is an associate professor at the Institut National de la Recherche Scientifique (INRS), Montreal, Canada. He was educated at the Technical University of Berlin, Germany, and received MSc and PhD degrees (both with distinctions) in 1998 and 2003, respectively. In the summer of 2003, he was a postdoc fellow at the Massachusetts Institute of Technology (MIT), Cambridge. He was a visiting professor at Stanford University, Stanford, October 2006 through March 2007. Dr. Maier is a co-recipient of the 2009 IEEE Communications Society Best Tutorial Paper Award. His research activities aim at rethinking the role of optical networks and exploring novel applications of optical networking concepts and technologies across multidisciplinary domains, with a particular focus on communications, energy, and transport for emerging smart grid applications and bimodal fiber-wireless (FiWi) networks for broadband access. He is the author of the book *Optical Switching Networks* (Cambridge University Press, 2008), which was translated into Japanese in 2009.